COMPARISON OF PREDICTIVE FIR-BASED ZERO-CROSSING DETECTION METHODS

Matti Pöllä

Helsinki University of Technology
Institute of Intelligent Power Electronics
P.O.Box 3000, FIN-02150 Espoo, FINLAND, Matti.Polla@hut.fi

ABSTRACT

Zero-crossings of sinusoidal signals are used for component synchronization especially in many applications in power electronics. Predictive finite impulse response (FIR) filters – bandpass filters with negative phase delay at a specific frequency – can be used to design a zero-crossing detector which operates without delay. Adaptation to frequency variations and computational simplicity have been the goals for various FIR implementations developed in recent years. An evaluative review of six such methods is presented in this article along with simulation results of their performance.

1. INTRODUCTION

Accurate zero-crossing detection of highly distorted sinusoidal signals is a requirement of several applications in power electronics. Especially in thyristor power converters where the zero-crossings are used for switching synchronization. The additional requirement of real-time filtering for these detectors makes the problem a non-trivial one.

An additional challenge is introduced by the slight variation in the nominal frequency of the line voltage signal (50 Hz $\pm$ 2%).

Several methods for delayless zero-crossing detection have been developed by Ovaska and Vainio [1–5]. They all share a structure based on a predictive FIR filter and differ from each other by the complexity of their implementation and the way of adaptation to the frequency variation.

However, the use of the predictive FIR-based filtering algorithms is not limited to switching synchronization in power converters. For example active power filtering is an area where prediction of sinusoidal signals has been applied successfully to reduce harmonics in power systems [6].

2. BASIC SCHEME

The simplest filtering method presented in [1] is formed of a median filter, a predictive FIR filter and an interpolator connected in cascade (Figure 1). All the other methods can be understood as improvements of this basic scheme.

The median filter is used to remove strong impulsive noise from the signal. For each time interval n, it selects

Figure 1. Block diagram of a predictive FIR-based zero-crossing detector.

the median of three successive input samples $x(n)$.

$$y(x) = \text{median}\{x(n-1), x(n), x(n+1)\} \qquad (1)$$

As the length of commutation notches in power converters is typically under 600 μs the sampling frequency (1.67 kHz) has been selected so that all impulsive disturbances fit inside a single sample. Thus all one-sample long disturbances are removed effectively. As a drawback a median filter with a window length of three samples adds a one-sample delay to the signal.

After the median filtering, the signal is filtered with an FIR filter that adds a two-sample forward phase shift to the signal. The prediction requirement for sine wave extrapolation is defined as

$$x(n+p) = \sum_{k=0}^{N-1} h(k)x(n-k) \qquad (2)$$

where $h(k)$ denotes the impulse response of the filter.

This can be achieved by designing a filter with a frequency response $H(e^{j\omega})$ which has the following characteristics:

$$|H(e^{j\omega_0})| = 1 \qquad (3)$$

$$\text{Arg}\left(H(e^{j\omega_0})\right) = -0.12\pi \qquad (4)$$

where ω_0 denotes the nominal frequency of the input signal (50 Hz).

The first requirement (3) states that the amplitude at the nominal frequency must not change. The second requirement (4) defines the correct phase shift to cause a two-sample advance.

An additional goal in the selection of the FIR coefficients is to minimize the noise gain defined as

$$\sum_{k=0}^{N-1} [h(k)]^2 \qquad (5)$$

This optimization task can be carried out analytically using the method of Lagrange multipliers [1].

In the final stage the signal is interpolated by a Lagrange interpolator to increase the time resolution of the output signal to 100 μs and thus a one-sample delay is added to the signal. As a result, the phase shift of the whole system at the nominal frequency is zero and the signal can be filtered with no phase shift (delay).

3. IMPROVED METHODS

All the succeeding filtering methods differ from the first one only by the predictive FIR part. The compared methods are Table lookup, LMS, general parameters (GP), multiplicative general parameters (MGP) and a simplified moving average version of the MGP algorithm (MGP-MA).

3.1. Table lookup

In the first improved method, the suitable coefficients for various nominal frequencies ($\omega_0 \pm 2\%$) are stored in a memory array. As the frequency changes, new coefficients can be loaded from the array [2]. This algorithm is an improvement to the basic scheme but requires a large memory and lacks true adaptivity.

3.2. LMS

In the LMS method the filter coefficients are adjusted by the Widrow-Hoff LMS algorithm. The coefficients are updated as

$$\vec{H}(n+1) = \vec{H}(n) + 2\mu e(n)\vec{x}(n-2) \tag{6}$$

where $\vec{H}(n) = [h(0), ..., h(N-1)]^T$ is the filter coefficient vector, $\vec{x} = [x(n-2), ..., x(n-N-1)]^T$ is the data vector in the filter window, $e(n)$ is the prediction error

$$e(n) = x(n) - \vec{H}^T(n)\vec{x}(n-2) \tag{7}$$

and μ is a small positive constant that determines the learning rate [3]. As a drawback this algorithm has the tendency to overly adapt to error signals as a consequence of many degrees of freedom in the adaptation.

3.3. GP

The general parameters method [4, 7] divides the filter coefficients to a fixed and an adjustable part. This way the adaptation of the filter can be limited to avoid adapting to error signals.

The output of the GP filter is defined as

$$y(n) = \sum_{k=0}^{N-1} [g(n) + h(k)]x(n-k) \tag{8}$$

where the general parameter is updated as

$$g(n+1) = g(n) + \gamma[r(n) - y(n)] \sum_{k=0}^{N-1} x(n-k) \tag{9}$$

where $r(n)$ is the reference input and γ is a gain factor.

With only two degrees of freedom in the adaptation the GP method is highly redundant against adaptation to error signals [4].

3.4. MGP

The MGP method is a computationally lighter version of the GP method. In the case of two general parameters the output is computed as

$$\begin{aligned} y(n) =& g_1(n) \sum_{k=0}^{N_1} h(k)x(n-k) \\ &+ g_2(n) \sum_{k=N_1+1}^{N-1} h(k)x(n-k) \end{aligned} \tag{10}$$

where the general parameters are updated as

$$g_1(n+1) = g_1(n) + \gamma e(n) \sum_{k=0}^{N_1} h(k)x(n-k) \tag{11}$$

$$g_2(n+1) = g_2(n) + \gamma e(n) \sum_{k=N_1+1}^{N-1} h(k)x(n-k) \tag{12}$$

where $e(n)$ is the prediction error and γ is a gain factor. N_1 is an integer in the interval $0 \leq N_1 \leq N-1$ that divides the filter in two blocks [5].

3.5. MGP-MA

With lower filter lengths, the general parameters alone can give good results. This allows an extremely simple implementation of an averaging filter (moving average) by setting the fixed filter coefficients to unity [5].

4. SIMULATIONS

The performance of the filtering algorithms was examined with extensive simulations. A highly distorted sinusoid (Figure 2) seen in a thyristor converter was modelled by adding impulsive disturbances, harmonic components and random noise to the pure sinusoid. Slight variation in the nominal frequency was taken into account by using three different test signals with nominal frequencies of 49, 50 and 51 Hz. All simulations were run on a 12 second long sample.

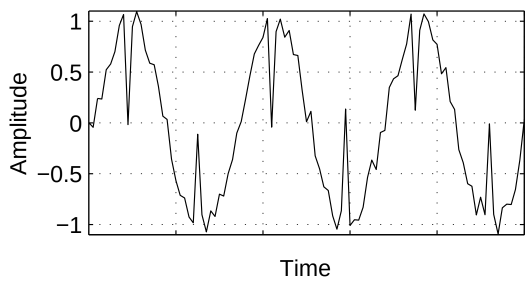

Figure 2. The test signal – a distorted 50 Hz sinusoid.

The zero-crossings defined by

$$x(n)x(n+1) \leq 0 \tag{13}$$

were recorded for a distorted signal and a pure sinusoid. The zero-crossing detection error can then be analyzed by looking at the absolute mean error and the standard deviation of the error. As a result we have a Gaussian-like distribution of the error (Figure 3). A good detection algorithm produces a narrow symmetric zero-centered distribution.

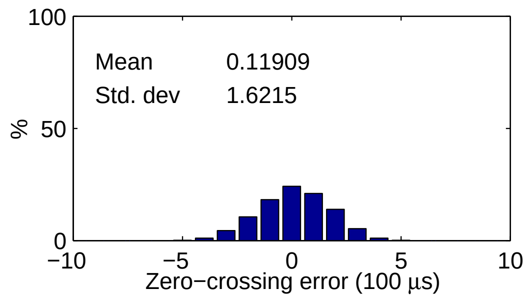

Figure 3. Zero-crossing error histogram.

The detection algorithms were implemented as described in the referred papers [1–5]. Filter length $N = 11$ was used for all methods except the Table lookup method with a filter lenght $N = 21$. Two general parameters were used in the GP-based algorithms.

The initial convergence of the LMS- and GP-based methods was taken into account by discarding the results produced before the adaptive parameters have converged.

5. RESULTS

The performance of the different zero-crossing methods can be compared by the absolute mean error (Figure 5) and the standard deviation of the error (Figure 6) at different frequencies. A small value is desirable for both the absolute mean error and the standard deviation of the error.

Simulations show that the basic scheme with a fixed coefficient set works very well for the nominal frequency of 50 Hz but fails at other frequencies because of the lack of frequency adaptation. For a 49 Hz signal the resulting histogram (Figure 4) is almost symmetric but centered slightly left of zero resulting a large value for the absolute mean error.

The exceptionally good result of the Table lookup method is caused by the longer filter length (N=21) and thus cannot be compared with the other methods directly. Although the simulation results are in favor of a long filter the length has disadvantages also. The prediction band is wider for short filters and the accuracy of the fixed coefficients in the general parameter-based algorithms is less critical for shorter filters [5].

The LMS and the GP methods both adapt to the frequency variation but introduce a slightly greater standard deviation in the zero-crossing error. This can be seen as a wide error histogram centered near zero.

The MGP method shows good performance in both comparisons at all frequencies and thus it can be ranked as the best zero-crossing detection method in these simulations. Even the simplified moving average version of the MGP algorithm shows a good result although its implementation is much less complex compared to the others.

6. REFERENCES

[1] O. Vainio and S. J. Ovaska, "Noise reduction in zero crossing detection by predictive digital filtering," *IEEE Trans. Industrial Electronics*, vol. 42, pp. 58–62, Feb. 1995.

[2] O. Vainio and S. J. Ovaska, "Digital filtering for robust 50/60 Hz zero crossing detectors," *IEEE Trans. Instrumentation and Measurement*, vol. 45, pp. 426–430, Apr. 1996.

[3] O. Vainio and S. J. Ovaska, "Multistage adaptive filters for in-phase processing of line-frequency signals," *IEEE Trans. Industrial Electronics*, vol. 44, pp. 258–264, Apr. 1997.

[4] S. J. Ovaska and O. Vainio, "General parameter-based adaptive extension to FIR filters," in *Proc. IEEE International Conference on Acoustics, Speech, and Signal Processing*, Salt Lake City, UT, May 2001, vol. 6, pp. 3765–3768.

[5] O. Vainio and S. J. Ovaska, "Adaptive lowpass filters for zero-crossing detectors," in *Proc. 28th Annual International Conference of the IEEE Industrial Electronics Society*, Sevilla, Spain, Nov. 2002, vol. 2, pp. 1483–1486.

[6] A. H. Samra and A. Teshome, "Current injection method to eliminate harmonics in AC power systems," in *Proc. IEEE Industrial and Commercial Power Systems Technical Conference*, Milwaukee, WI, May 1993, pp. 85–91.

[7] A. A. Ashimov and D. J. Syzdykov, "Identification of high-dimensional system by the general parameter method," in *Preprints 8th IFAC World Congress*, Kyoto, Japan, Aug. 1981, pp. 32–37.

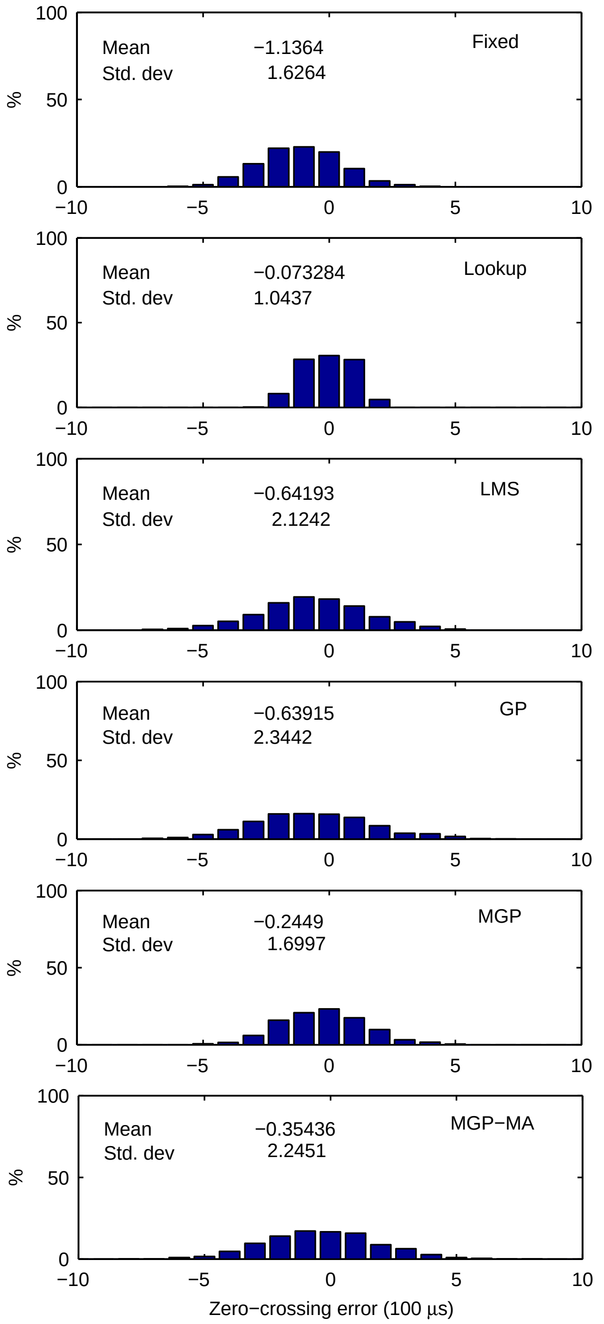

Figure 4. Zero-crossing error distributions for a 49 Hz test signal.

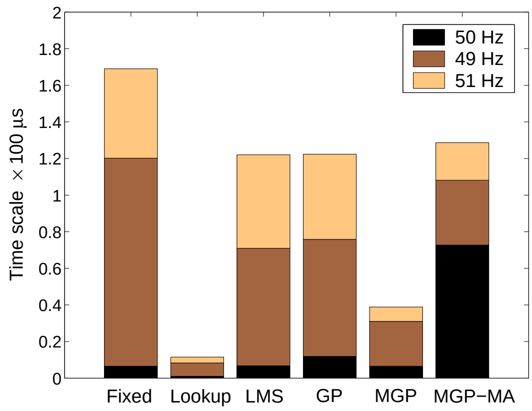

Figure 5. Comparison of the absolute value of the mean error.

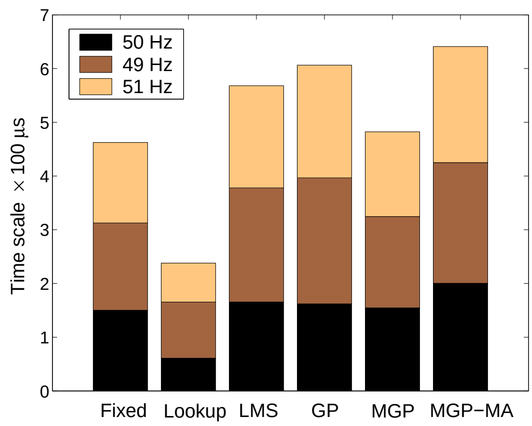

Figure 6. Comparison of zero-crossing error standard deviation.